

**Screening Level Assessment of Risks Due to Dioxin Emissions
from Burning Oil from the BP Deep Water Horizon Gulf of Mexico Spill
Supporting Information**

John Schaum^{1}, Mark Cohen³, Steven Perry², Richard Artz³, Roland Draxler³, Jeffrey B. Frithsen¹, David Heist², Matthew Lorber¹, and Linda Phillips¹*

¹U.S. EPA, Office of Research and Development, Washington, DC

²U.S. EPA, Office of Research and Development, RTP, NC

³NOAA, Air Resources Laboratory, Silver Spring, MD

*Corresponding author e-mail: schaum.john@epa.gov; phone (703) 347- 8623; fax (703) 347-8690

BURN DATA

The Supplementary Materials includes a spreadsheet summarizing the oil burn data. These data were originally collected by BP and the Coast Guard and are presented here with permission from BP. For purposes of the modeling in this paper, these data were modified by Daewon Byun and Hyun Cheol Kim (NOAA Air Resources Laboratory, Silver Spring, MD) in the following ways: 1) missing lat/longs were replaced by oil well location, 2) missing burn durations were replaced from volume/duration regressions, 3) missing starting times were replaced with 2 pm local time and 4) burn #289 was removed as no information was provided.

AERMOD MODELING

Effect of wind speed: It was no surprise with these very hot plumes that near-surface concentrations were very small for the light wind (1 m/s) cases. Plume rise can be hundreds of meters in light winds and until the plume rise is arrested by more stable layers aloft or sufficient ambient mixing, the pollutants can be very slow to reach the surface and only then in relatively low concentrations. With increased winds, the plumes are more bent over and dispersion caused

by both plume-generated turbulence and atmospheric turbulence can more effectively mix pollutant material to the surface. However, even for these high wind cases, the plume rise with distance downwind is significant and the concentrations tend to decrease rapidly with distance. Since some of the rising plume may penetrate into the elevated stable layers, this material will eventually diffuse back to the surface and may result in slight increases in concentration with distance. This slight increase effect, while not important in the current risk analysis, is seen with all cases for downwind distances between 2,000 and 2,500 meters. Finally, based on the nearest buoy measurements the wind speeds (adjusted to a two-meter height) did not exceed 6 m/s during the actual burn periods. Winds were less than 5 m/s during almost 90% of the hours involving burns.

Effect of mixing height: While mixing height has a secondary effect (compared to wind speed) on the surface concentrations, it shows its effect in two ways. As the plumes rise through the mixed layer and into the elevated stable layer, their rate of rise will be slowed. Unlike in the HYSPLIT modeling where the final plume rise was used we chose the very conservative assumption in the AERMOD modeling exercise that the fraction of the rising plume that penetrates into the elevated stable layer would only rise up to an additional 10% of the mixed layer depth. Eventually, this plume material in the stable layer will diffuse back to the surface and affect distant concentrations, although in a small way because the plumes are so well diffused at this point. Maximum surface concentration reported in Table 1 occurs at a downwind distance where the rising plume has not interacted with the elevated stable layer.

Effect of emission factor: With all else assumed constant the ambient concentrations estimated by AERMOD scale linearly with the emission factor. For example, if the emission factor was set to 1.7 ng TEQ/kg oil burned as found by Aurell and Gullett (1) for measurements in moderate to small sized fires, the concentrations shown in Table 1 would reduce proportionately (i.e., the maximum near surface concentration for 10 m/s winds at 50 meters downwind from the fire would reduce to 2.6 from 4.6 pg TEQ/m³ in Table 1). Therefore, assuming that the congeners below detection limits are equal to their full detection limit is another conservative assumption.

Comparison of model estimates to plume observations: During the period of July 13 through 16, 2010, Aurell and Gullett (1) collected samples to estimate dioxin concentrations within the plumes of 27 burns. Their samples were collected approximately 200 to 300 meters

downwind of the burns with plume heights from 75 to 200 meters. We examined the distribution of burn rates and meteorology associated with those particular burns. The wind speeds ranged from 1 to 6 m/s and the estimated emission rates ranged from about 2 to 7×10^{-2} $\mu\text{g TEQ}/\text{sec}$. AERMOD was applied to this specific subset of burn and meteorological conditions. The AERMOD simulated in-plume concentrations at the heights and downwind locations of the measurements ranged from 0.17 to 0.54 $\text{pg TEQ}/\text{m}^3$ while the composite sampling over all 27 burns estimated the in-plume concentration to be 0.2 $\text{pg TEQ}/\text{m}^3$. While only a limited spatial comparison, this level of agreement between model estimates and observations lends confidence to the screening analysis estimates of worst case worker exposures.

HYSPLIT MODELING

Simulation Results Grid and Illustrative Sites.

The locations of the grid-square centroids in the HYSPLIT-SV simulation-results grid, along with 14 illustrative sites in the region, are shown in Figure S-1.

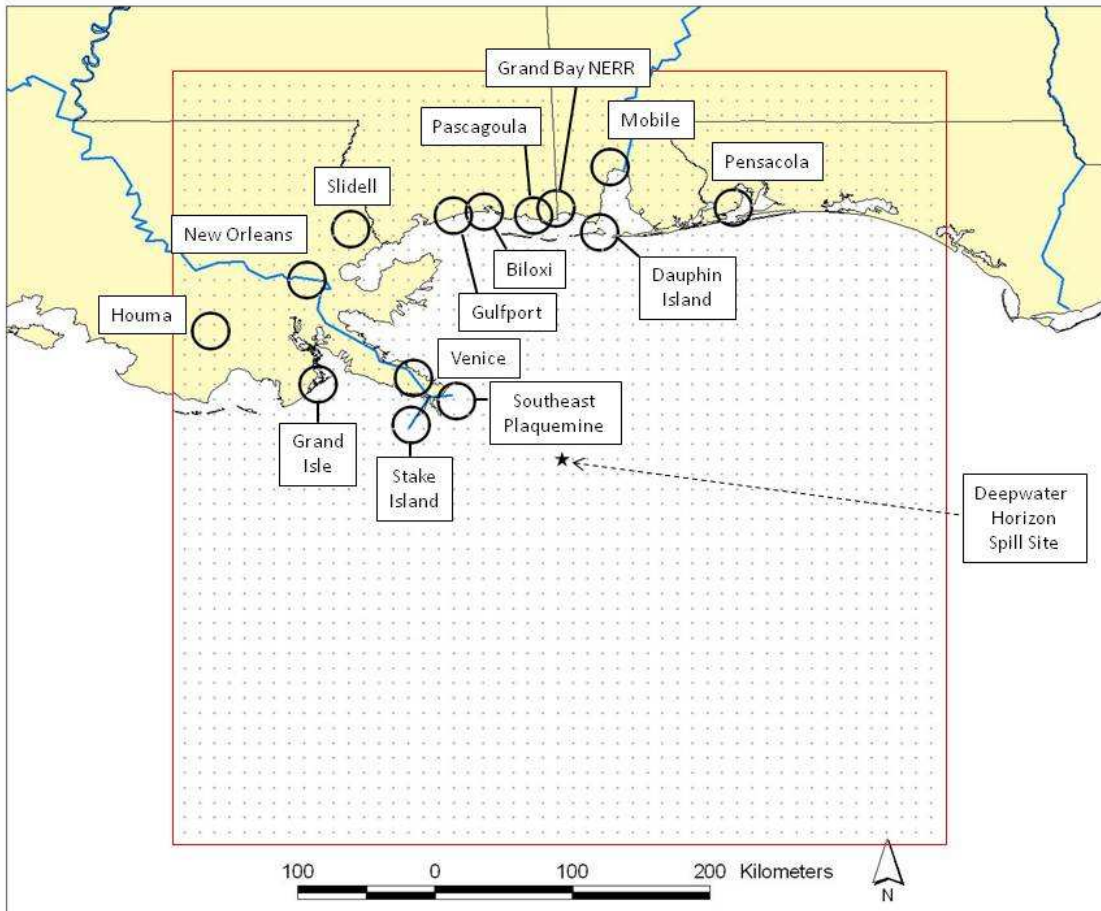


Figure S-1. HYSPLIT simulation results grid and 14 illustrative locations in the vicinity of the Deepwater Horizon site.

Episodicity of Modeled Oil Burn Impacts.

As mentioned in the main paper, due to the variations in meteorological conditions (e.g., wind speed and direction) and intermittent nature of the burns, the deposition flux and atmospheric concentrations at any given location – even from the simulated continuous emissions – are highly variable or “episodic”. As an illustration of this phenomenon, Figure S-2 shows the time series of hourly modeled surface-level (10 m) air concentrations for a subset of the 14 illustrative regional locations shown in Figure 1, for a 16-day period in June 2010. This period was shown because it had the some of the highest modeled surface-level air concentrations, and the subset of sites includes only those sites that had significant model-estimated concentrations during this period. It can be seen that the concentrations are highly episodic; the concentration peaks occur at different times in different locations, and the magnitude of the peaks is highly variable.

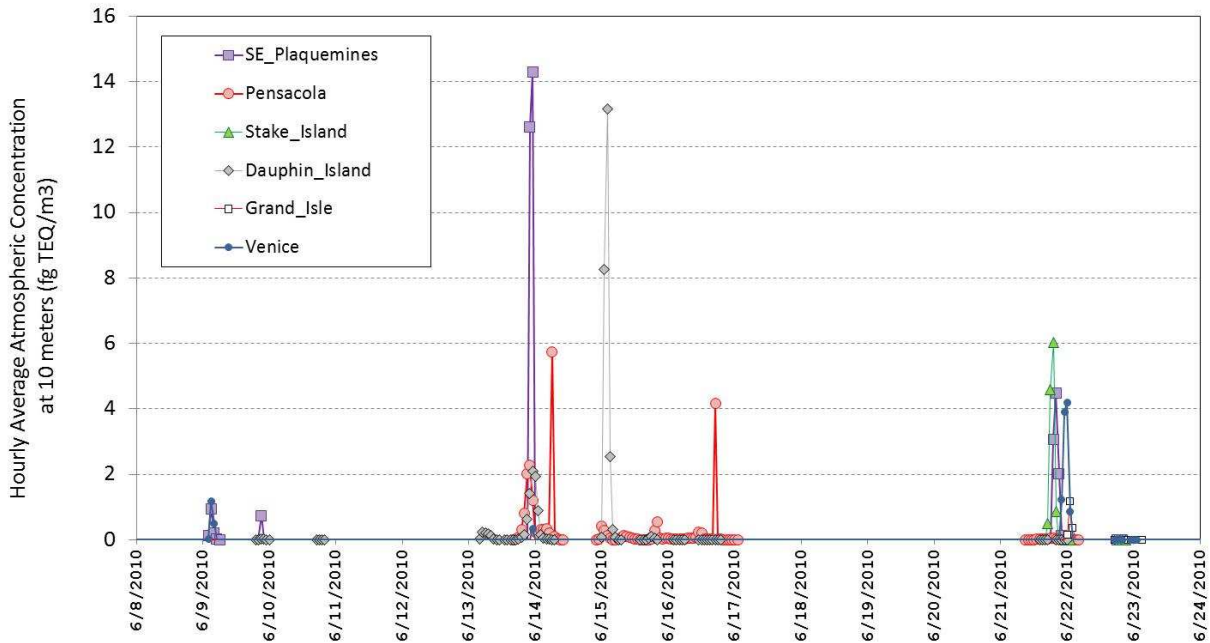


Figure S-2. Time series of modeled PCDD/F concentrations (at 10 meter elevation) at several illustrative locations in the Gulf of Mexico region resulting from estimated dioxin emissions from reported burn events.

Concentration Results for 14 Illustrative Regional Sites.

In Figures S-3 and S-4, the overall average and maximum hourly average concentrations for the entire modeling period are shown, respectively, for each of the 14 illustrative locations shown in Figure 1.

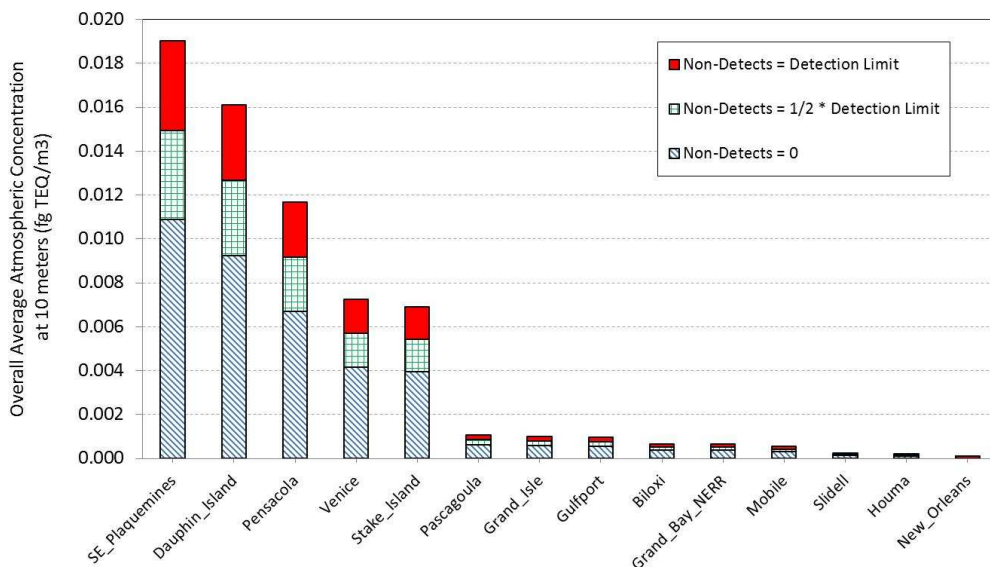


Figure S-3. Average modeled concentrations at 10 meter elevation for the entire modeling period at 14 selected locations in the Gulf of Mexico region. The maximum values (representing emissions estimated assuming non-detected congeners were present at the detection limit) are the same data tabulated in the Figure 1 caption in the main paper.

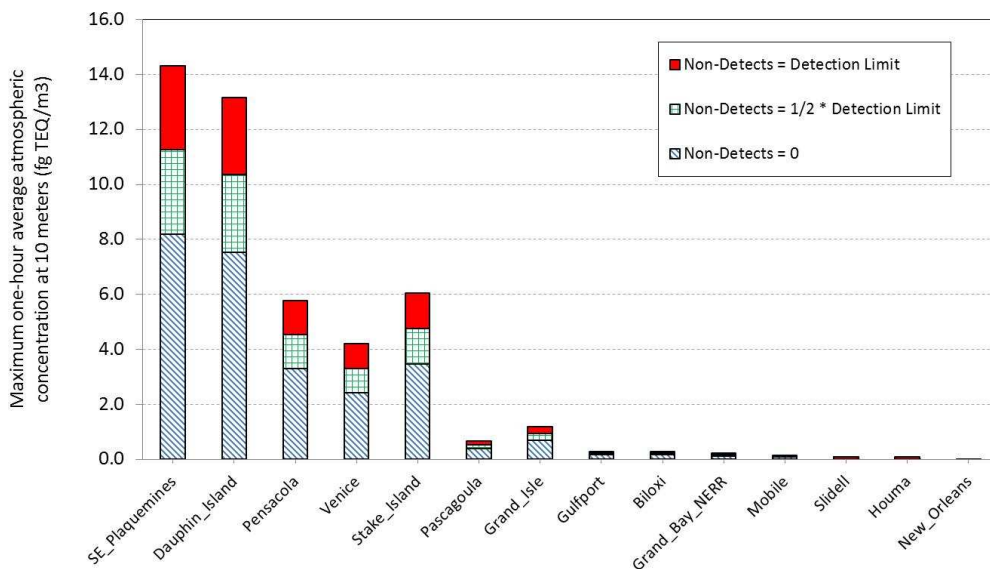


Figure S-4. Maximum modeled one-hour average concentrations at 10 meter elevation for the entire modeling period at 14 selected locations in the Gulf of Mexico region.

Maximum 24-hr Average Concentrations for the Entire Simulation Results Grid.

In the main paper, Figure 1 shows the average modeled ground level concentration over the entire modeling period April 28 -- July 22, 2010 for each grid square. Figure S-5 shows the *maximum 24-hour-average*, modeled ground-level (10 m) concentrations for each grid square over the same period. The highest 24-hr-average modeled shoreline (or inland) concentrations was 0.92 fg TEQ/m^3 , and this occurred at the grid square with centroid latitude /longitude of $30.2367 / -87.7872$ (near the Bon Secour National Wildlife Refuge).

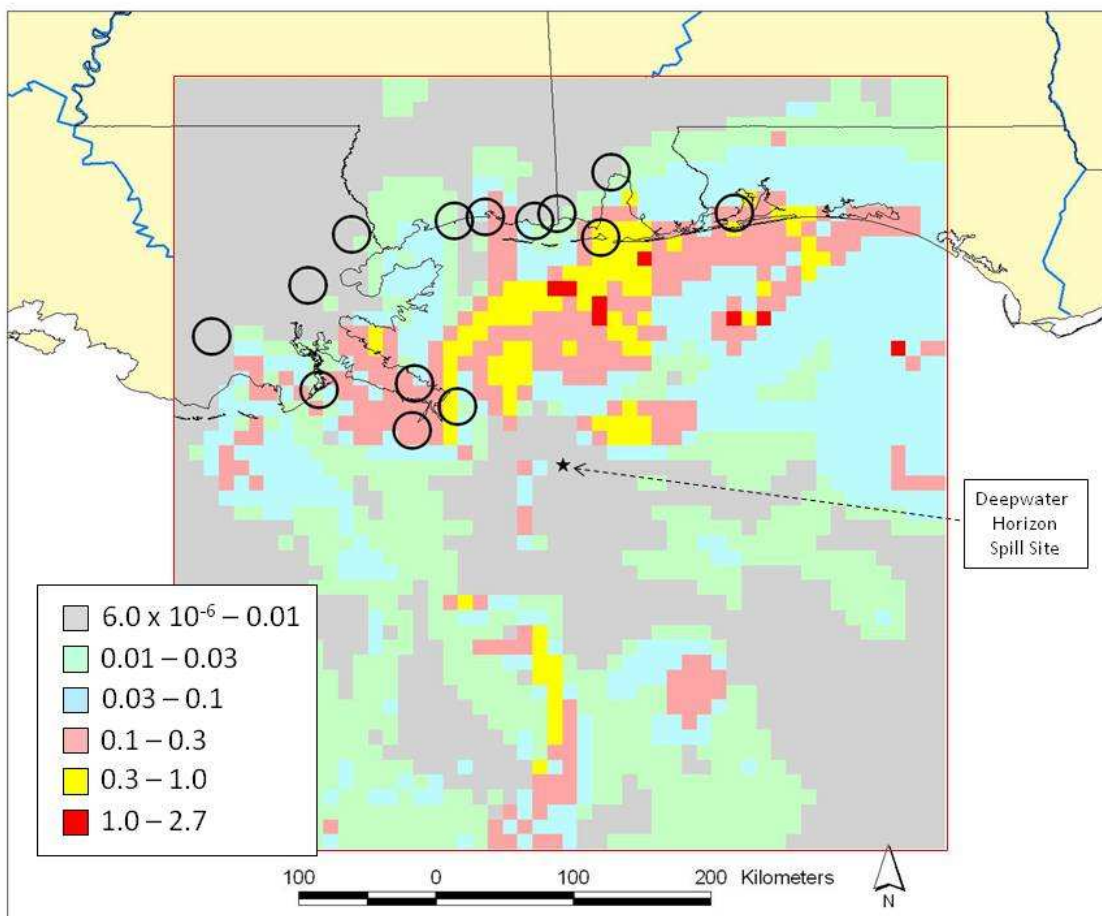


Figure S-5. Maximum modeled 24-hr average ground-level concentrations (fg TEQ/m³) for each grid square over the entire modeling period April 28 – July 22, 2010.

Sensitivity of Results to Plume Rise Estimates.

To investigate the sensitivity of the results to assumptions regarding plume rise, a simulation was done for 2,3,7,8-TCDD setting the final plume rise height to be 200 m for all burn events -- as opposed to estimating the plume rise based on the characteristics of each burn and the accompanying meteorological conditions during each burn. Presentation and discussion of these and other sensitivity analyses are beyond the scope of this paper. However, as an example of the results, the average concentration of 2,3,7,8-TCDD at the SE Plaquemines illustrative site increased by approximately a factor of 3 if a final plume rise height of 200 m was assumed for each burn, rather than using the model-estimated plume rise. The likely reason for this change is that for at least some of the larger burning events – for which plume rise might be expected to be relatively higher, with all other factors being equal – the assumption of 200 m final height may have been a significant underestimate. This would influence the ground level concentrations downwind of the burn, and as seen in this example, the ground-level concentration at this particular shoreline location of 2,3,7,8-TCDD would be increased by approximately a factor of 3 if the plume rise were assumed to be the same value of 200m for each burn event. Analogous comparisons could be performed for other congeners.

Concentration as a Function of Distance from the Spill Site.

Grid cells were divided into categories based on the distance between their centroid and the spill site: 0-25 km, 25-50 km, 50-75 km, ... up to largest range of 225-250 km.

Concentration: Figure S-6 shows that the average modeled concentration [averaged over all directions] was largest in the distance range 100-125 km from the spill site. Figure S-7 shows that the distance ranges with the highest single grid-square average concentrations are 125-150 km, 150-175 km, and 225-250 km. This figure just represents the values of the grid cell in a given distance range that has the highest average concentration over the modeling period. As noted in the main paper, the highest, modeled grid-cell overall average 10m concentration was 0.051 fg TEQ/m³, and this occurred at a grid cell approximately 125 km northeast from the spill site.

Deposition: Figure S-8 shows the average modeled PCDD/F deposition flux (fg TEQ/m²) in each of the different distance ranges away from the spill site. It can be seen that the largest average deposition flux occurs in the range 50-75 km away from the spill site. Figure S-9 shows the total modeled PCDD/F deposition (ug TEQ) in different distance ranges away from the spill site. The geographical distribution shown in this figure differs from that of Figure S-8. This is because while the flux decreases significantly at large distances from the site, the area over which this flux occurs increases. Thus, Figure S-9 shows that the while the total deposition maximum also occurs in the distance range 50-75 km away from the spill site, the deposition amounts do not drop off as significantly at further distances. Figure S-10 shows the same data as Figure S-9, except that the deposition totals have been normalized by the total estimated emissions from the oil burning activities (0.134 g TEQ). It can be seen that approximately 4% of the total emissions were deposited in the range 50-75 km away from the spill site. Approximately 26% of the emissions (on a TEQ basis) were deposited with 250 km of the spill site.

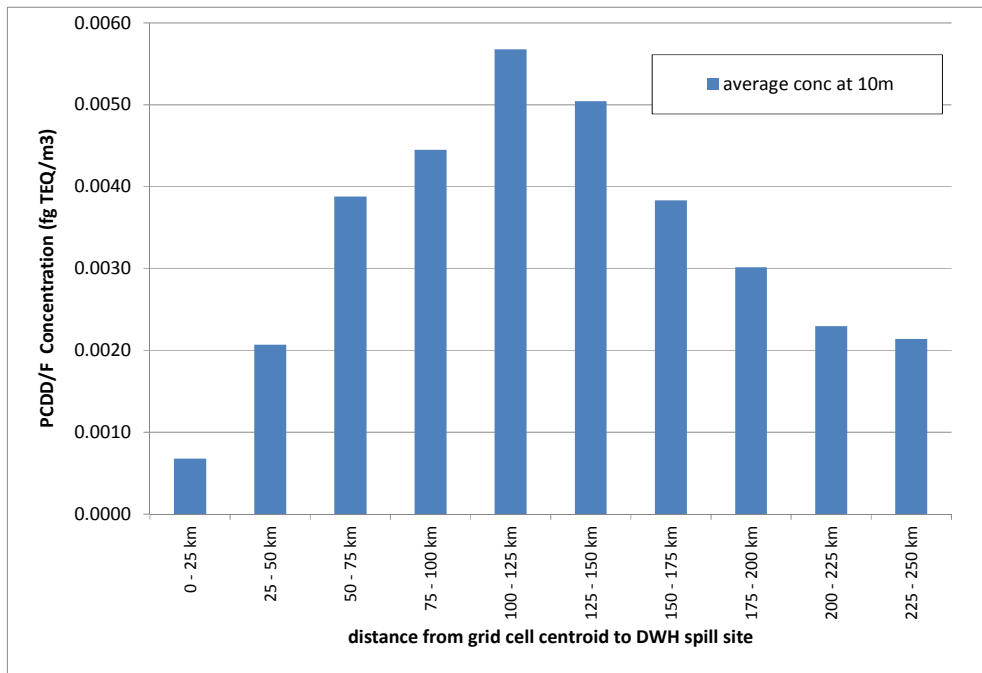


Figure S-6. Average concentration as a function of distance range from the DWH spill site for grid squares, over the entire modeling period April 28 – July 22, 2010.

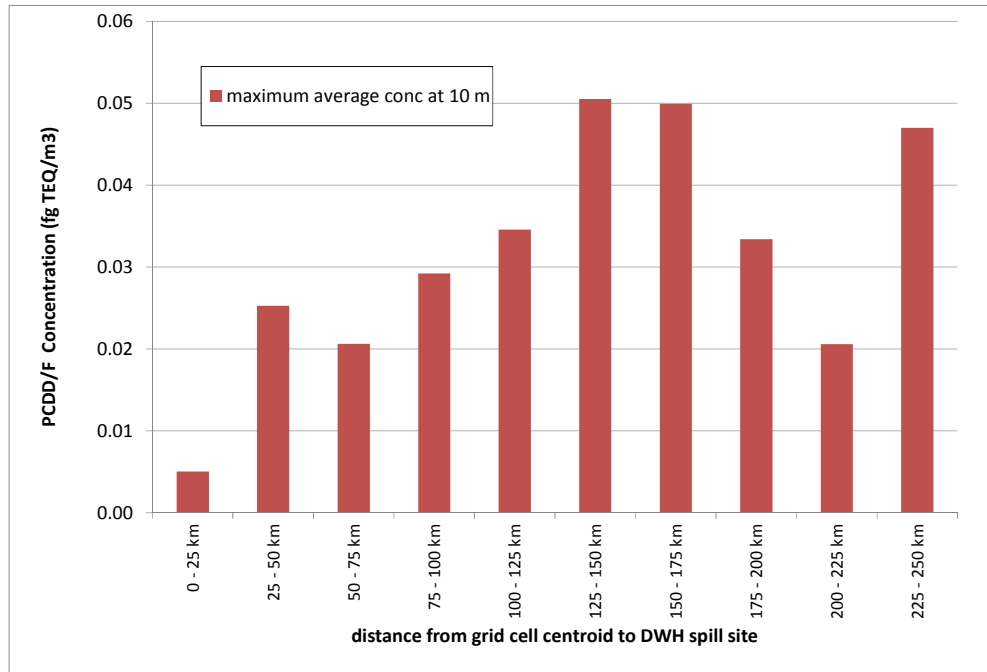


Figure S-7. Maximum grid-square average concentration as a function of distance range from the DWH spill site, over the entire modeling period April 28 – July 22, 2010.

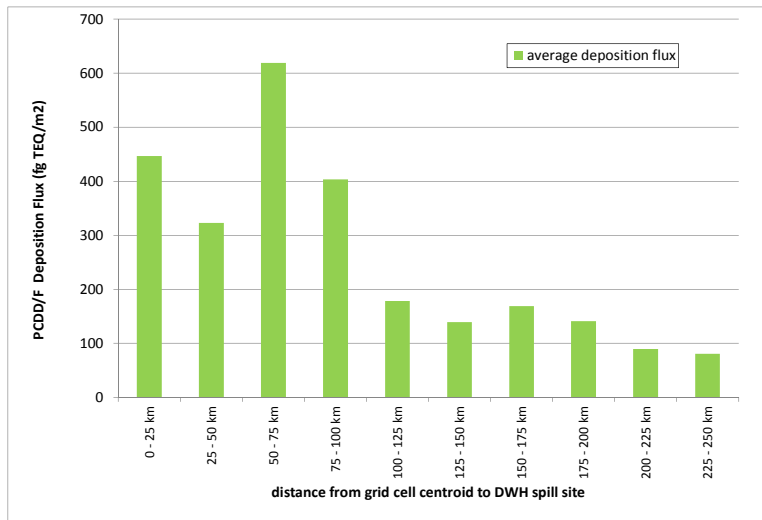


Figure S-8. Average PCDD/F deposition flux (fg TEQ/m²) in different distance ranges from the DWH spill site, over the entire modeling period April 28 – July 22, 2010.

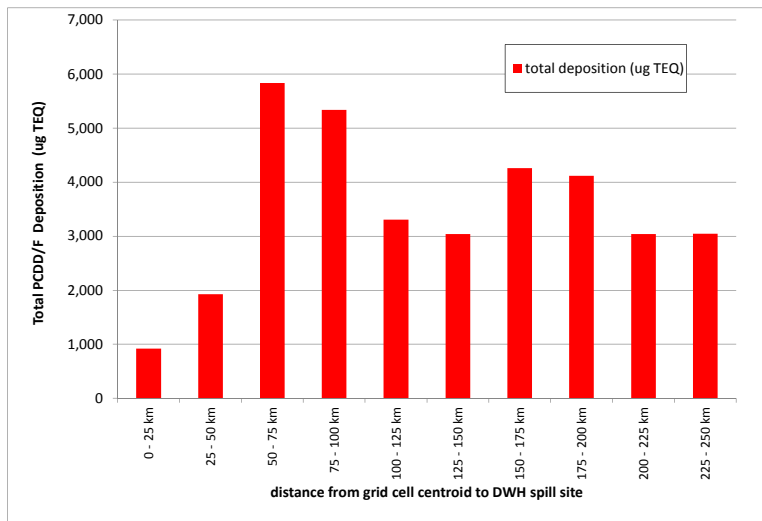


Figure S-9. Total PCDD/F deposition flux (ug TEQ) in different distance ranges from the DWH spill site, over the entire modeling period April 28 – July 22, 2010.

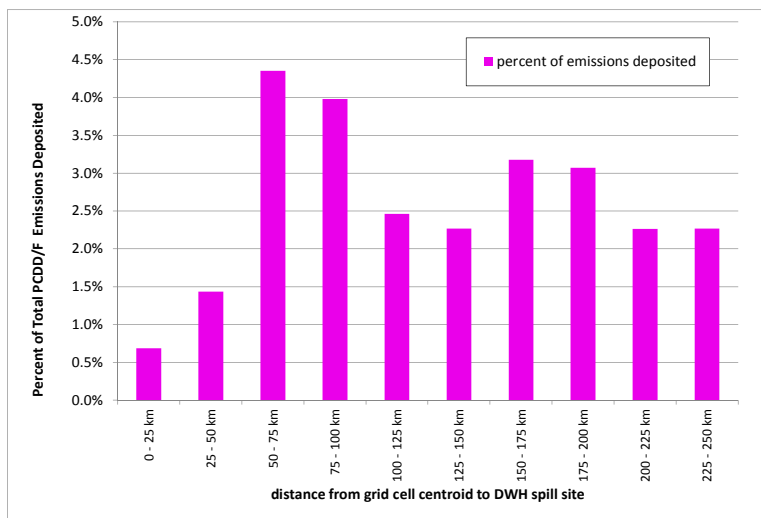


Figure S-10. Percent of total PCDD/F emissions from oil burning deposited in different distance ranges from the DWH spill site, over the entire modeling period April 28 – July 22, 2010. Summing up all of the bars, the modeling estimated that a total of 26% of the total emissions were deposited within 250 km of the DWH spill site, on a TEQ basis.

Modeled Deposition Mass Balance for Different Congeners

A deposition mass balance analysis was performed for each of the seventeen 2,3,7,8-substituted congeners simulated with the HYSPLIT-SV model over the entire modeling domain (shown in Figure S-11). Note that the modeling domain shown in Figure S-11 is larger than the concentration-deposition results grid presented elsewhere in this analysis. Figure S-12 shows the fraction of total modeled deposition (over the entire modeling domain shown in Figure S-11) accounted for by dry deposition, for both the vapor phase and the particle phase. For each congener, wet deposition accounted for the remaining fraction of total deposition. For example, for 2,3,7,8-TCDD, approximately 30% of the emitted deposited mass was dry deposited in the vapor phase, about 2% was dry deposited in the particle phase, and the remaining 68% was wet deposited. The relative importance of different deposition pathways appears to be consistent with the expected vapor/particle partitioning behavior of the different congeners. In Figure S-13, the total deposition (on a TEQ basis) over the entire modeling domain is presented for each modeled congener. Note that since the TEQ emissions factor for OCDD was zero, the modeled TEQ deposition for this congener is also zero. It can be seen that the most important congeners contributing to deposition (on a TEQ basis) over the entire domain were 1,2,3,7,8-PeCDD and 2,3,4,7,8-PeCDF. Wet deposition was the most important deposition pathway for each of these two congeners. In Figure S-14, the fraction of the total emissions deposited over the entire modeling domain is shown for each congener. It can be seen that approximately 40% of the total emissions were deposited in the modeling domain for each congener.

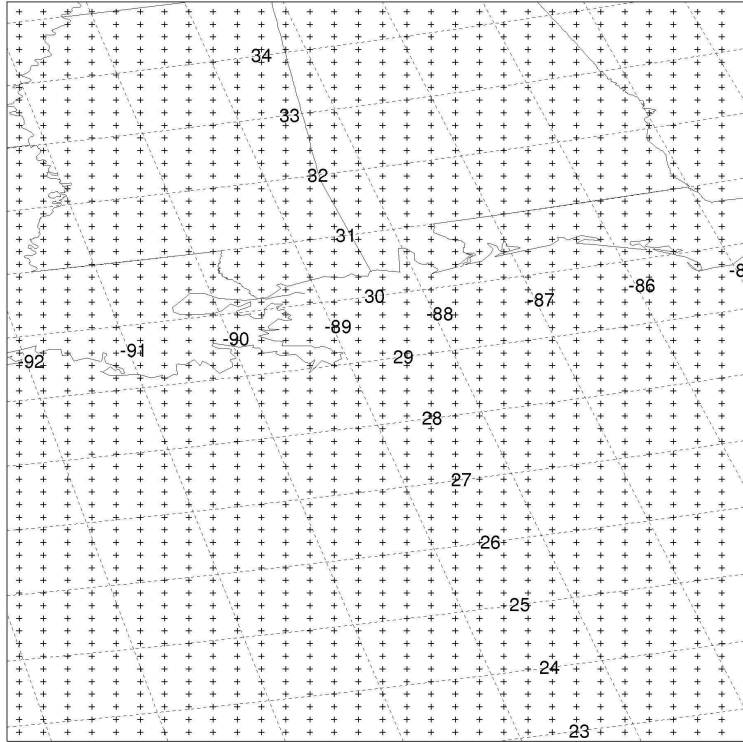


Figure S-11. Overall HYSPLIT-SV modeling domain on which the mass balance results of this section are based.

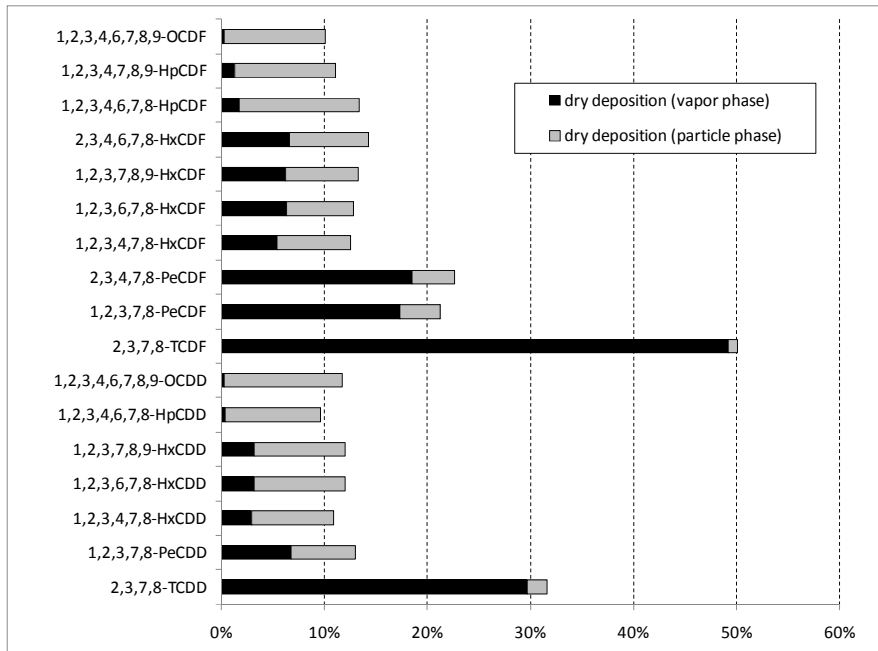


Figure S-12. Percent of total modeled deposition for a given congener over the modeling domain simulated to be dry deposited. For each congener, the remaining deposition was through wet deposition processes.

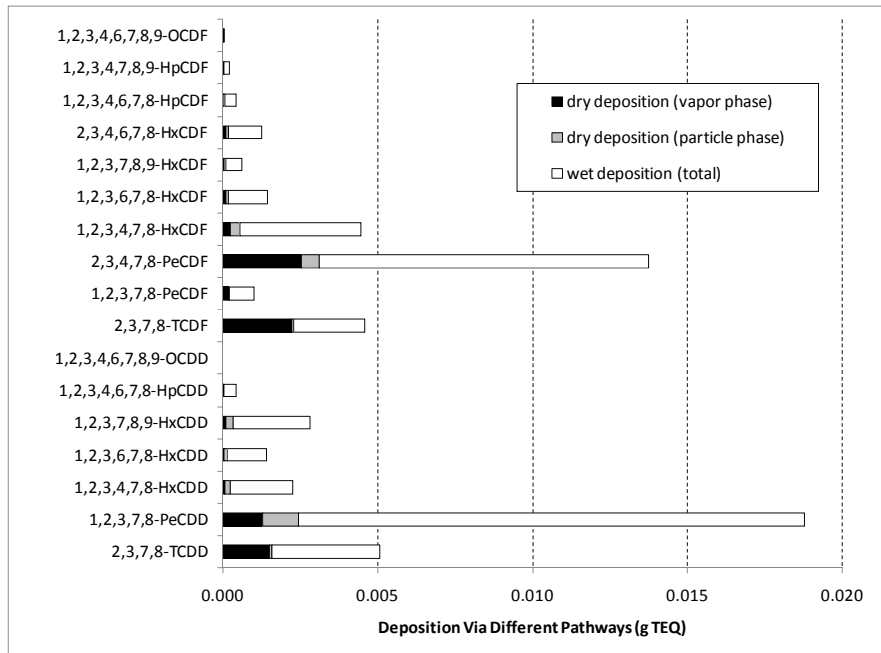


Figure S-13. Total deposition of each congener over the entire modeling domain, using the model inputs as described in the main paper, e.g., upper end of range of amount of oil burned and assuming congeners not detected during the emissions testing were present at their detection limit.

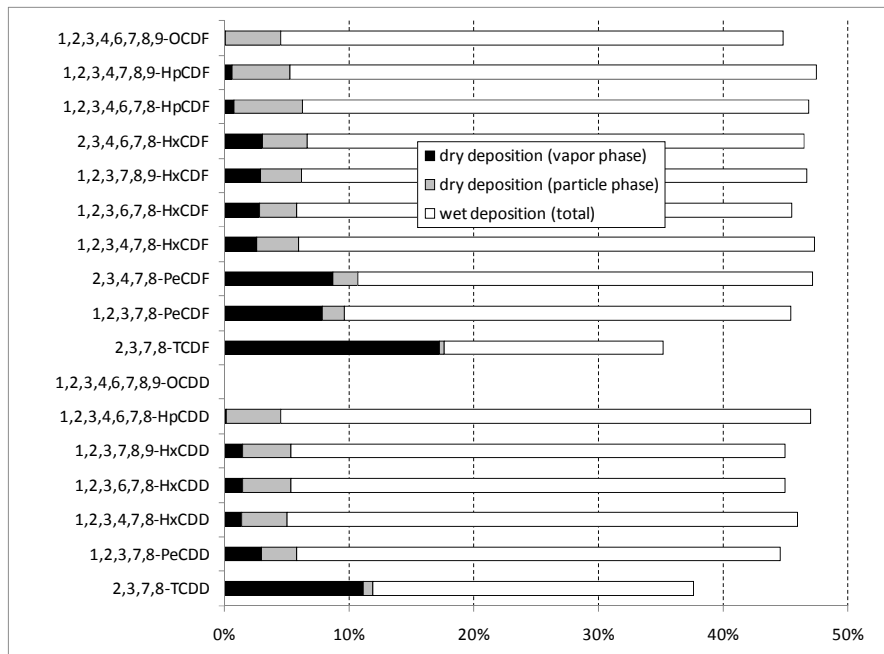


Figure S-14. Fraction of the total emissions of each congener deposited over the entire modeling domain.

FISH MODELING

Fish Uptake Approach

The fish uptake of dioxin from atmospheric deposition has been studied in the Baltic Sea by Vikelsoe et al. (2). They used measurements of the content of dioxin in fatty pelagic fish (herring and salmon) and an estimation of the yearly production of biomass in the Baltic Sea to derive a fish uptake fraction of 0.004 (or 0.4%). This represents the fraction of dioxin flux deposited into the sea from the atmosphere which is taken up in fish. Uptake fractions in the Gulf of Mexico are likely to be different due to differences such as temperature, depth, and dominant fish species. However, since this was the most relevant data that could be found, an analysis was conducted to explore how these data could be used to predict fish concentrations from the oil burn deposition and compare them to those predicted using bioaccumulation factors. Accordingly, this uptake fraction was used to estimate fish concentrations as follows:

$$C_F = DEP * UF / CR \quad (S-1)$$

Where:

C_F = fish concentration, pg TEQ/g

DEP = deposition of dioxin into Gulf during burn period, pg TEQ/m²

UF = fish uptake fraction, unitless

CR = catch rate during burn period, g/m²

This model assumes that a portion of the dioxin depositing over the 3-month burn is taken up in the fish catch during this period. The dioxin deposition rate represents the total deposition from all of the oil burns. This was set to 10,000 fg TEQ/m², or 10 pg TEQ/m², based on HYSPLIT modeling results. The fish uptake fraction was set to 0.004 (or 0.4%) on the basis of a study by Vikelsoe et al. (2).

The fish catch rate was estimated as follows. In 2008, the commercial fish and shellfish harvest from the five U.S. Gulf states was estimated to be 590 million kg/yr and the recreational fish harvest in 2008 was 33 million kg/yr (3). Therefore, the total catch is estimated to be 623 million kg/yr. The Gulf measures approximately 1,600 km from east to west, 900 km from north

to south, and has a surface area of 1.4 million km² (4). For purposes of deriving an average fish catch rate, it was assumed that all fishing occurred within 100 km of shore which is estimated to be approximately 20% of the total area (0.28 million km²). Dividing the fish catch by the area where fishing was assumed to occur, suggests an average catch rate of 2,200 kg/km²-yr (or 2.2 g/m²-yr). As a form of validation, the catch rate of 2,200 kg/km²-yr was compared to the annual primary production of the Gulf of Mexico. The Gulf is considered a Class II, moderately productive (150-300 gC/m²-yr), ecosystem based on SeaWiFS global primary productivity estimates (5). This is equivalent to a range of 150,000 kg/km²-yr to 300,000 kg/km²-yr. Generally, fish production is less than 1% of primary production rates (6). Based upon the estimated primary production rate, fish production should be no more than 1,500 to 3,000 kg/km²-yr. The estimate of 2,200 kg/km²-yr falls within this range. The fish catch during the three month burn time would be one fourth of this amount or 550 kg/km².

Finally the fish concentration was calculated using Equation S-1. Assuming a deposition rate of 10 pg TEQ/m², an uptake fraction of 0.004, and a catch rate of 550 kg/km², the resulting fish tissue concentration was 0.073 pg TEQ/g.

The BSSAF Approach

In this approach, fish tissue concentrations are estimated based on the sorbed phase concentration in suspended sediments of the water column, rather than the dissolved phase. The equation is advocated for dioxins in EPA's Dioxin Reassessment (7):

$$C(\text{lipid}) = C(\text{oc}) * \text{BSSAF} \quad (\text{S-2})$$

Where:

C(lipid) = fish lipid concentration, pg/g

C(oc) = organic carbon concentration in suspended sediment, pg/g

BSSAF = biota suspended sediment accumulation factor, unitless

EPA (7) describes the application of this model and assigns a value of 0.07 to BSSAF for 2,3,7,8-TCDD. For simplicity, that value will be assumed to apply to dioxin TEQ.

The concentration in organic carbon of suspended sediment is calculated as the concentration in suspended sediment divided by the fraction of organic carbon in the sediment.

First, the concentration on suspended sediments must be calculated. A total concentration was given as 0.001 pg TEQ/L. Carranza-Edwards et al (8) provide a value of 5 mg/L as the concentration of suspended sediment in the Gulf of Mexico. The paper assumes 10% of the total water concentration is in the soluble phase, with 90% in the sorbed phase. Given a suspended sediment concentration of 5 mg/L and this 90% assumption, the concentration of TEQ in suspended sediment is solved as 0.18 pg TEQ/g, as follows:

$$[0.0009 \text{ (90\% of 0.001) pg/L} * 1000 \text{ L/m}^3] \div [5 \text{ mg/L} * 0.001 \text{ g/mg} * 1000 \text{ L/m}^3]$$

EPA (7) assumes that suspended sediment is 5% organic carbon, and if it is assumed that all dioxin is sorbed to the organic carbon fraction of suspended sediment (which is reasonable given the affinity of dioxin-like compounds to organic carbon), the final C(oc) for use in Equation (S-2) is, 3.6 pg TEQ/g (0.18 pg TEQ/g ÷ 0.05).

Finally, substituting this value in Equation (S1) along with a 0.07 for BSSAF results in a fish lipid concentration prediction of 0.25 pg TEQ/g lipid. If one assumes edible fish to be 7% lipid (7), then a final fish concentration is 0.018 pg TEQ/g whole fish (0.25 pg TEQ/g lipid * 0.07). This compares to 0.024 pg TEQ/g whole fish estimated using the BAF approach and 0.073 pg/g using the fish catch approach.

References

1. Aurell, J.; Gullett, B.K. Aerial sampling of PCDD/PCDF emissions from the Gulf oil spill *in situ* burns. Submitted to *Environ. Sci. Technol.* **2010**.
2. Vikelsøe, J.; Andersen, H.V.; Bossi, R.; Johansen, E.; Chrillesen, M. Dioxin in the Atmosphere of Denmark. A Field Study at Selected Locations. NERI Technical Report No. 565.
http://www2.dmu.dk/1_viden/2_Publikationer/3_fagrappporter/rapporter/FR565.PDF
2005.
3. U.S. EPA. Gulf of Mexico Program, General Facts about the Gulf of Mexico
<http://www.epa.gov/gmpo/about/facts.html>). Dated May 17, 2010. **2010a**.
4. **Gulfbase.org. General Facts about the Gulf of Mexico 2010.**
<http://www.gulfbase.org/facts.php>

5. The Encyclopedia of Earth. Gulf of Mexico large marine ecosystem. **2008**.
http://www.eoearth.org/article/Gulf_of_Mexico_large_marine_ecosystem
6. Houde, E.D.; Rutherford, E.S. Recent Trends in Estuarine Fisheries: Predictions of Fish Production and Yield. *Estuaries* **1993**, 16(2), 161-176.
7. US EPA. Exposure and Human Health Reassessment of 2,3,7,8-Tetrachlorodibenzo-p-Dioxin (TCDD) and Related Compounds. United States Environmental Protection Agency, Office of Research and Development, National Center for Environmental Assessment. NAS Review Draft. **December, 2003**. EPA/600/P-00/001C(a-f). Available at, <http://www.epa.gov/ncea/dioxin.htm>.
8. Carranza-Edwards, A.; Rosales-Hoza, L.; Monreal-Gómez, A. Suspended sediments in the southeastern Gulf of Mexico. *Marine Geology*, **1993**, 112, 257-269.